Study of non-linear evolution of the hadron structure within QCD

Štěpán Mayer

Supervisor: Jan Čepila
Consultant: Marek Matas

DUCD24
September 19, 2024

Structure of hadrons

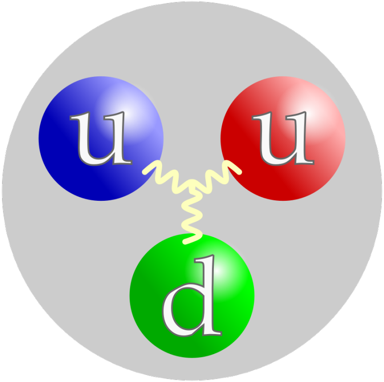

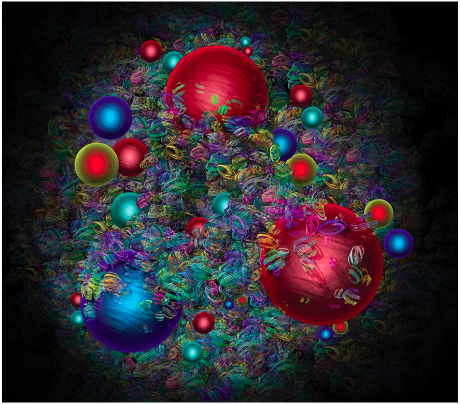

Structure of hadrons

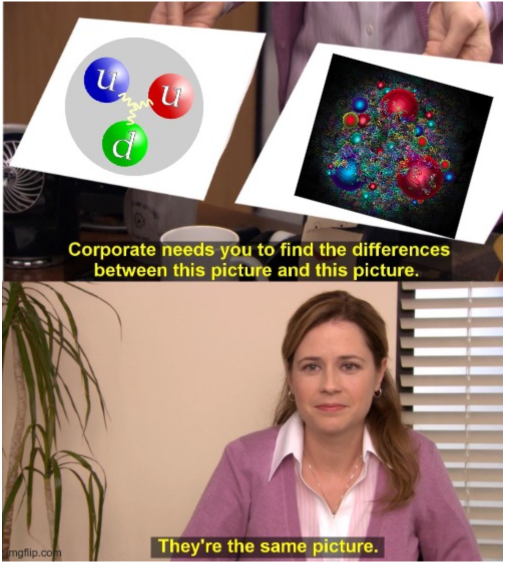

Deep-inelastic scattering

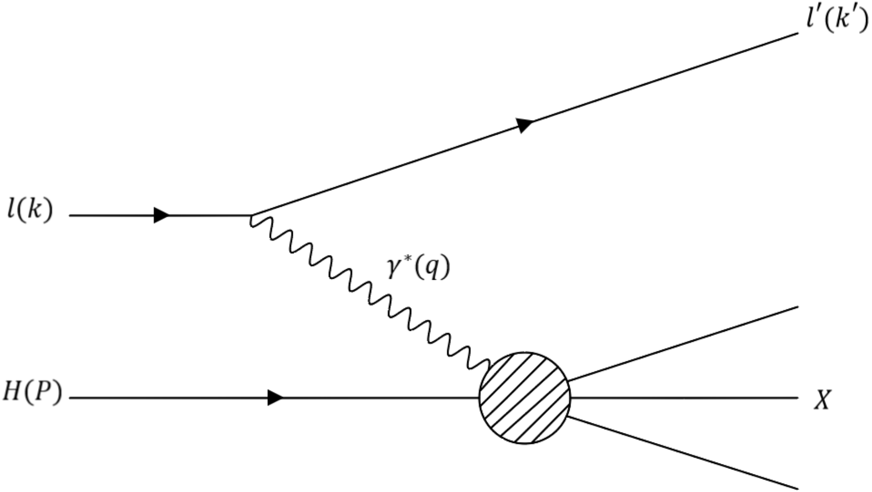

Parton model

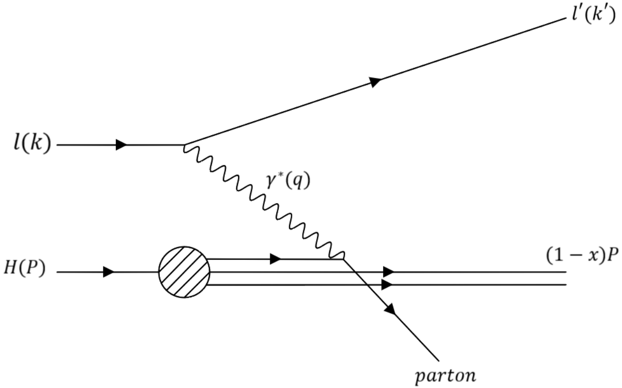

- Hadrons consist of free, spin-half, point-like *partons*
- Bjorken-x: Fractional momentum carried away by the parton within DIS

Color dipole model

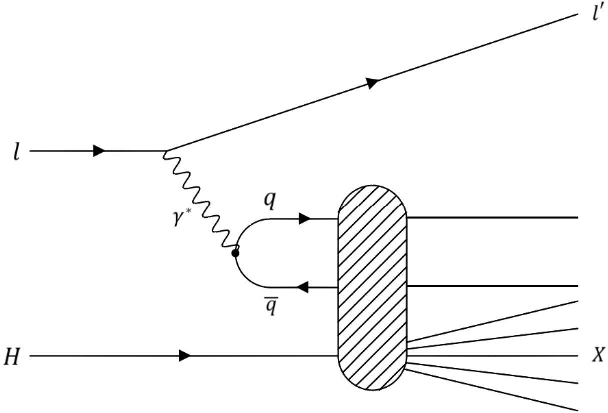

- Fock expansion and taking the simplest fluctuation

Evolution of parton densities

- Parton distribution functions $f_i(x, Q^2)$
- 2 evolution directions
- Balitsky-Fadin-Kuraev-Lipatov (BFKL) equation

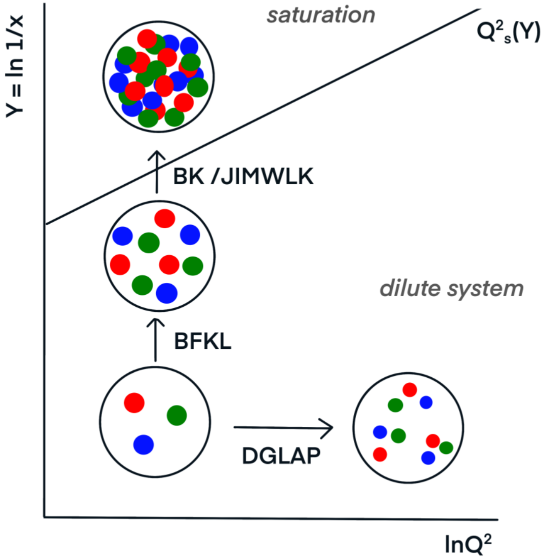

Parton saturation

- No limit on the number of partons with BFKL $\rightarrow$ violates unitarity of PDFs
- New non-linear effect to dominate low-x
- PDFs must saturate at a certain value
- Saturation represents a balance between emission and recombination of partons

Color glass condensate

- = Field theory model of high-energy limit of QCD
- CGC is used to describe the saturation region
- BFKL $\rightarrow$ Jalilian-Marian-Iancu-McLerran-Wüsthoff-Leonidov-Kovner (JIMWLK) equations
- JIMWLK equations = set of infinite coupled equations $\rightarrow$ no known analytical solution exists

Approximations to JIMWLK

- Limit of large N_C $\rightarrow$ neglect the parts of JIMWLK with $(N_C)^{-\alpha}$, $\alpha \geq 2$
- We can assume the emission of a gluon to be equivalent to the emission of a color dipole of size $r \sim 0$

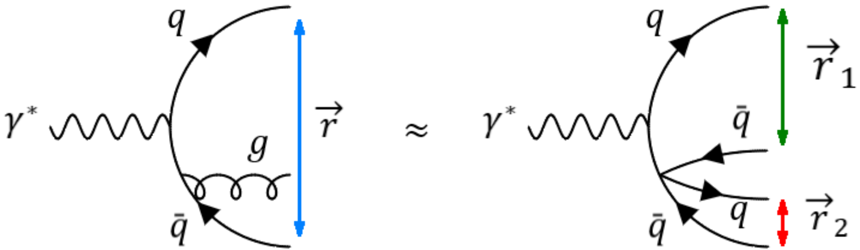

Balitsky-Kovchegov (BK) equation

- Evolution of dipole scattering amplitudes $N(\vec{r}, Y)$ with rapidity (Bjorken-x) $Y = \ln\left(\frac{1}{x}\right)$
- Focussed on impact-parameter independent form
- Due to geometry: $r_2 = \sqrt{r^2 + r_1^2 - 2rr_1 \cos\varphi}$

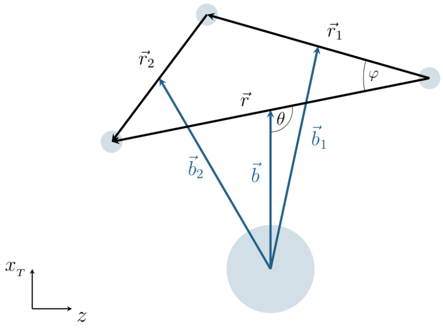

Balitsky-Kovchegov (BK) equation

- Impact-parameter independent form at projectile rapidity Y:

$$\frac{\partial N(\vec{r}, Y)}{\partial Y} = \int d^2 r_1 K(\vec{r}, \vec{r}_1, \vec{r}_2)$$
$$\left[N(\vec{r}_1, Y) + N(\vec{r}_2, Y) - N(\vec{r}, Y) - N(\vec{r}_1, Y) N(\vec{r}_2, Y)\right]$$

- Impact-parameter independent form at target rapidity η:

$$\frac{\partial N(\vec{r}, \eta)}{\partial \eta} = \int d^2 r_1 K_{ci}^{\eta}(\vec{r}, \vec{r}_1, \vec{r}_2)$$
$$\left[N(\vec{r}_1, \eta - \delta_{r_1}) + N(\vec{r}_2, \eta - \delta_{r_2}) - N(\vec{r}, \eta) - N(\vec{r}_1, \eta - \delta_{r_1}) N(\vec{r}_2, \eta - \delta_{r_2})\right]$$

The kernel

- BFKL kernel with fixed coupling

$$K_{BFKL}(\vec{r}, \vec{r}_1, \vec{r}_2) = \frac{\alpha_s N_C}{2\pi^2} \frac{r^2}{r_1^2 r_2^2}$$

The kernel

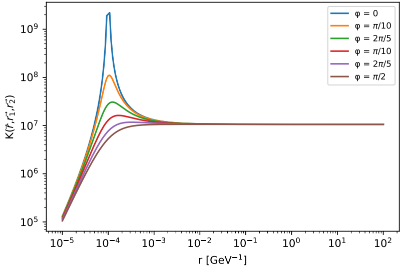

Figure: The BFKL kernel with fixed coupling at $\alpha_s = 0,7$, $r_1 = 0,0001$ GeV^{-1} and different values of φ.

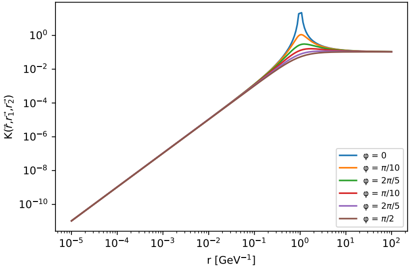

Figure: The BFKL kernel with fixed coupling at $\alpha_s = 0,7$, $r_1 = 1$ GeV^{-1} and different values of φ.

The kernel

- Kernel incorporating the running of the coupling

$$K_{rc}(\vec{r},\vec{r}_1,\vec{r}_2) = \frac{\alpha_s(r^2)N_C}{2\pi^2}\left[\frac{r^2}{r_1^2 r_2^2} + \frac{1}{r_1^2}\left(\frac{\alpha_s(r_1^2)}{\alpha_s(r_2^2)} - 1\right) + \frac{1}{r_2^2}\left(\frac{\alpha_s(r_2^2)}{\alpha_s(r_1^2)} - 1\right)\right]$$

$$\alpha_s(r^2) = \frac{4\pi}{(11 - \frac{2}{3}N_f)\ln\left(\frac{4C^2}{r^2\Lambda_{n_f}^2}\right)}$$

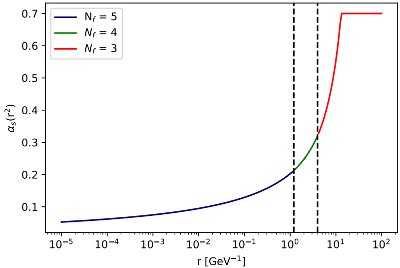

The kernel

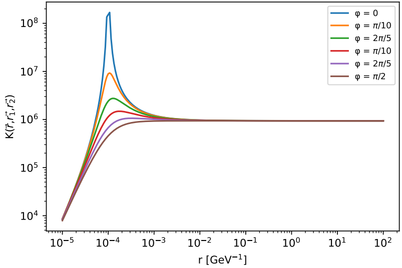

Figure: The kernel incorporating the running of the coupling with $r_1 = 0,0001$ GeV^{-1} at different values of φ.

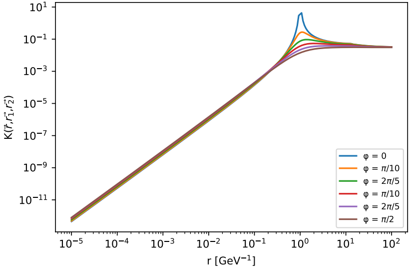

Figure: The kernel incorporating the running of the coupling with $r_1 = 1$ GeV^{-1} at different values of φ.

The kernel

- Collinearly improved kernel

$$K_{ci}(\vec{r}, \vec{r}_1, \vec{r}_2) = \frac{\overline{\alpha}_s}{2\pi} \left[\frac{r^2}{r_1^2 r_2^2} \left(\frac{r^2}{\min(r_1^2, r_2^2)} \right)^{\overline{\alpha}_s A_1} \frac{J_1(2\sqrt{\overline{\alpha}_s |\ln(r_1^2/r^2)\ln(r_2^2/r^2)|})}{\sqrt{\overline{\alpha}_s |\ln(r_1^2/r^2)\ln(r_2^2/r^2)|}} \right]$$

$$\overline{\alpha}_s = \frac{N_C}{\pi} \alpha_s(\min(r^2, r_1^2, r_2^2))$$

The kernel

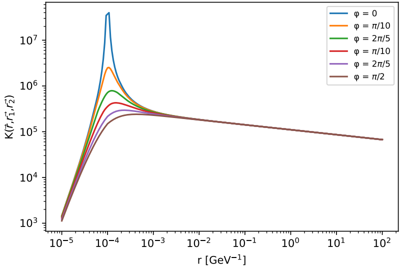

Figure: The collinearly improved kernel with $r_1 = 0,0001$ GeV^{-1} at different values of φ.

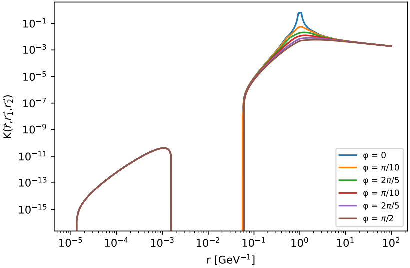

Figure: The collinearly improved kernel with $r_1 = 0,1$ GeV^{-1} at different values of φ.

The kernel

- Collinearly improved kernel at target rapidity

$$K_{ci}^{\eta}(\vec{r}, \vec{r}_1, \vec{r}_2) = \frac{\overline{\alpha}_s}{2\pi} \frac{r^2}{r_1^2 r_2^2} \left(\frac{r^2}{\min(r_1^2, r_2^2)} \right)^{\overline{\alpha}_s A_1}$$

The kernel

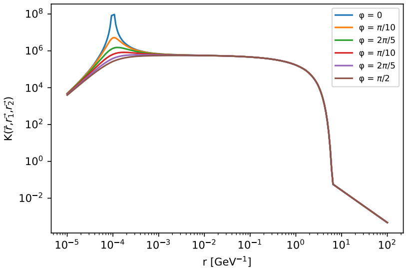

Figure: The collinearly improved kernel at target rapidity K_{ci}^{η} with $r_1 = 0,0001$ GeV^{-1} at different values of φ.

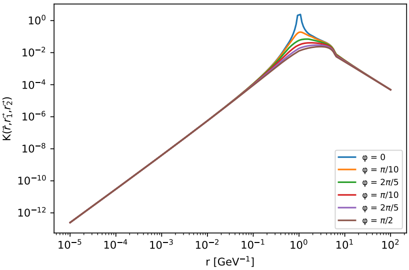

Figure: The collinearly improved kernel at target rapidity K_{ci}^{η} with $r_1 = 0,1$ GeV^{-1} at different values of φ.

Initial conditions - GBW model

$$N_{rc}^{GBW}(\vec{r}, Y = 0) = 1 - \exp\left(-\frac{(r^2 Q_{s_0}^2)^{\gamma}}{4}\right)$$

- With $\gamma = 0,971$, $Q_{s_0}^2 = 0,241$ GeV^2, $C = 2,46$, $\alpha_0 = 0,7$

$$N_{ci}^{GBW}(\vec{r}, Y = 0) = \left[1 - \exp\left(-\frac{(r^2 Q_{s_0}^2)^{\gamma}}{4}\right)^{p}\right]^{\frac{1}{p}}$$

- Where $p = 2,802$, $Q_{s_0} = 0,428$ GeV, $C = 2,358$ and $\alpha_0 = 1$

Initial conditions - MV model

$$N_{rc}^{MV}(\vec{r}, Y=0) = 1 - \exp\left[-\frac{(r^2 Q_{s_0}^2)^{\gamma}}{4} \ln\left(\frac{1}{r\Lambda_{QCD}} + e\right)\right]$$

- With $Q_{s_0}^2 = 0,165$ GeV^2 $\gamma = 1,135$, $C = 2,52$ and $\alpha_0 = 0,7$

$$N_{ci}^{MV}(\vec{r}, Y=0) = \left[1 - \exp\left(-\left[\frac{r^2 Q_{s_0}^2}{4}\overline{\alpha}_s(r^2)\left(1 + \ln\left(\frac{\overline{\alpha}_0}{\overline{\alpha}_s(r^2)}\right)\right)\right]^p\right)\right]^{\frac{1}{p}}$$

- Where $\overline{\alpha}_0 = \frac{N_C}{\pi}\alpha_0(r^2)$, $\alpha_0 = 1$, $C = 2,586$ and $p = 0,807$

Initial conditions - target rapidity

$$N(\vec{r}, \eta_0) = \left(1 - e^{-\left(\frac{r^2 Q_0^2}{4} \overline{\alpha}_s(r)\left(1 + \ln \frac{\overline{\alpha}_s^{max}}{\overline{\alpha}_s(r)}\right)\right)^p}\right)^{\frac{1}{p}}$$

- With Q_0 = 0.561 GeV, $C = 5,66$, $p = 1,76$ and $\overline{\alpha}_s^{max} = 1$

Solving the impact-parameter independent BK with Runge-Kutta methods

$$I_0 \equiv \int_0^{2\pi} d\varphi \int dr_1 r_1 K(r, r_1, r_2)$$

$$I_1 \equiv \int_0^{2\pi} d\varphi \int dr_1 r_1 K(r, r_1, r_2) \left[N(r_1, Y) + N(r_2(r, r_1, \varphi), Y) \right]$$

$$I_2 \equiv \int_0^{2\pi} d\varphi \int dr_1 r_1 K(r, r_1, r_2) N(r_1, Y) N(r_2(r, r_1, \varphi), Y)$$

$$f\left(Y, N(r, Y)\right) = I_1 - N(r, Y) I_0 - I_2$$

$$N(r, Y+h) = N(r, Y) + hf(N(r, Y)) + \frac{h^2}{2} f(N(r, Y))(I_0 - I_1) - \frac{h^3}{2} f^2(N(r, Y)) I_0$$

The results

- Solved on a logarithmic grid in r for 225 points between 10^{-5} GeV^{-1} and 10^{2} GeV^{-1} (same grid for r_1)
- Used a linear grid in φ for 11 points between 0 and π
- Step in rapidity of $h = 0,01$
- $N(r, Y)$ from RK
- $N(r_1, Y)$ same as $N(r, Y)$ (same grid)
- $N(r_2, Y)$ obtained by interpolation (Lagrange interpolation)

The results

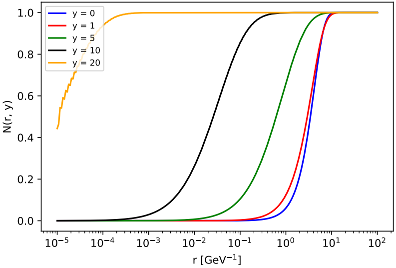

Figure: The resulting dipole scattering amplitudes evolving the GBW initial conditions with K_{BFKL}, showing the results of evolution for values of rapidity at $Y = 0$, $Y = 1$, $Y = 5$, $Y = 10$ and $Y = 20$.

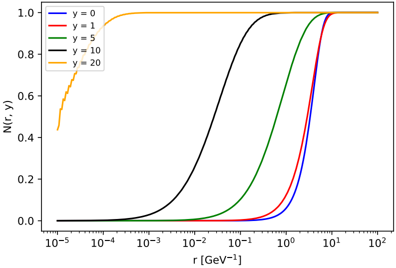

Figure: The resulting dipole scattering amplitudes evolving the MV initial conditions with K_{BFKL}, showing the results of evolution for values of rapidity at $Y = 0$, $Y = 1$, $Y = 5$, $Y = 10$ and $Y = 20$.

The results

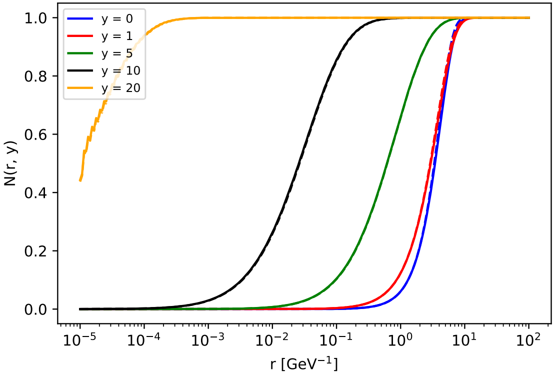

Figure: Comparing the results of dipole scattering amplitudes evolving different initial conditions GBW (full lines) and MV (dashed lines) with the same kernel K_{BFKL}, showing the results of evolution for values of rapidity at $Y = 0$, $Y = 1$, $Y = 5$, $Y = 10$ and $Y = 20$.

The results

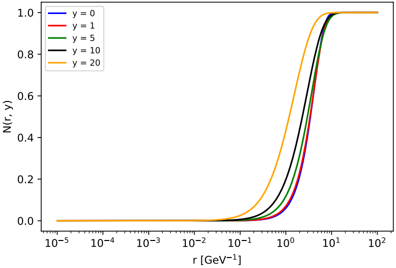

Figure: The resulting dipole scattering amplitudes evolving the GBW initial conditions with K_{rc}, showing the results of evolution for values of rapidity at $Y = 0$, $Y = 1$, $Y = 5$, $Y = 10$ and $Y = 20$.

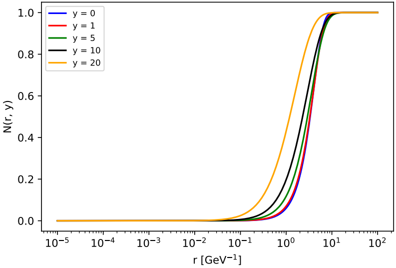

Figure: The resulting dipole scattering amplitudes evolving the MV initial conditions with K_{rc}, showing the results of evolution for values of rapidity at $Y = 0$, $Y = 1$, $Y = 5$, $Y = 10$ and $Y = 20$.

The results

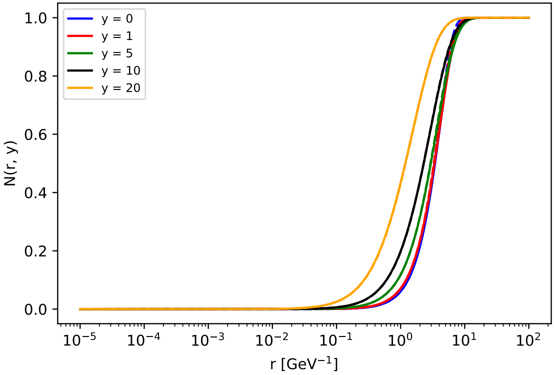

Figure: Comparing the results of dipole scattering amplitudes evolving different initial conditions GBW (full lines) and MV (dashed lines) with the same kernel K_{rc}, showing the results of evolution for values of rapidity at $Y = 0$, $Y = 1$, $Y = 5$, $Y = 10$ and $Y = 20$.

The results

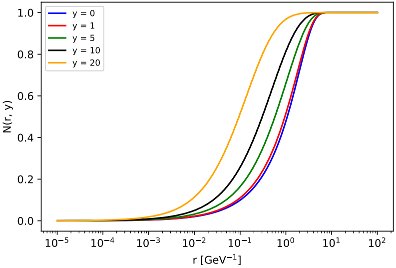

Figure: The resulting dipole scattering amplitudes evolving the GBW initial conditions with K_{ci}, showing the results of evolution for values of rapidity at $Y = 0$, $Y = 1$, $Y = 5$, $Y = 10$ and $Y = 20$.

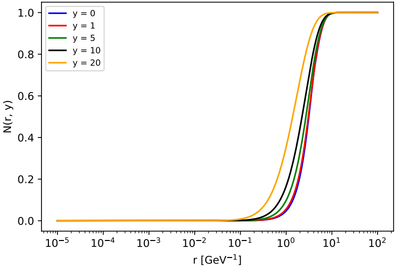

Figure: The resulting dipole scattering amplitudes evolving the MV initial conditions with K_{ci}, showing the results of evolution for values of rapidity at $Y = 0$, $Y = 1$, $Y = 5$, $Y = 10$ and $Y = 20$.

The results

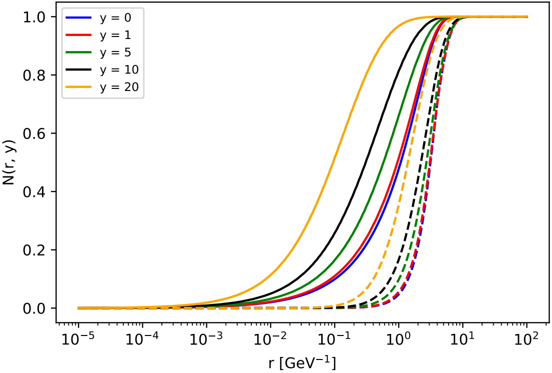

Figure: Comparing the results of dipole scattering amplitudes evolving different initial conditions GBW (full lines) and MV (dashed lines) with the same kernel K_{ci}, showing the results of evolution for values of rapidity at $Y = 0$, $Y = 1$, $Y = 5$, $Y = 10$ and $Y = 20$.

The results

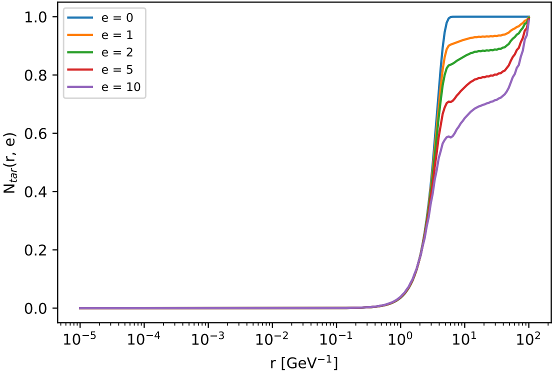

Figure: The resulting dipole scattering amplitudes for the BK equation at target rapidity, showing the results of evolution for values of rapidity at $\eta = 0$, $\eta = 1$, $\eta = 2$, $\eta = 5$ and $\eta = 10$.

Summary

- Deep inelastic scattering
- Saturation and evolution equations
- Balitsky-Kovchegov equation